CDC5 was also necessary for efficient phosphorylation of Mam1 (fig. S6). Thus, *CDC5* was required for Mam1 phosphorylation and localization to kinetochores.

Our data show that *CDC5* is required for (i) cleavage and removal of cohesin from chromosome arms at the onset of anaphase I, (ii) sister-kinetochore coorientation during meiosis I, and (iii) Cdc14 release from the nucleolus and anaphase I spindle disassembly. Cdc5 is likely to phosphorylate Rec8, thereby targeting it for cleavage, and probably causes anaphase I spindle disassembly by promoting the release of Cdc14 from the nucleolus. Cdc5 controls sister-kinetochore coorientation by promoting the localization of Mam1 to kinetochores, perhaps in part through phosphorylating Mam1. Although our data show that *CDC5* is a key regulator of meiosis I, the protein kinase may collaborate with meiosis-specific factors such as Spo13 to accomplish this task. Spo13 is required for sister-kinetochore coorientation and to inhibit cohesin cleavage (*28–30*). Together, these two proteins may modulate the mitotic chromosome segregation machinery to bring about the specialized meiosis I chromosome segregation program.

References and Notes

1. B. H. Lee, A. Amon, *Curr. Opin. Cell Biol.* **13**, 770 (2001).
2. K. Nasmyth, *Annu. Rev. Genet.* **35**, 673 (2001).
3. J. Y. Lee, T. L. Orr-Weaver, *Annu. Rev. Cell Dev. Biol.* **17**, 753 (2001).
4. A. Toth *et al.*, *Cell* **103**, 1155 (2000).
5. F. Klein *et al.*, *Cell* **98**, 91 (1999).
6. G. Sharon, G. Simchen, *Genetics* **125**, 475 (1990).
7. _____, *Genetics* **125**, 487 (1990).
8. S. Herrmann, I. Amorim, C. E. Sunkel, *Chromosoma* **107**, 440 (1998).
9. D. Chase *et al.*, *Genesis* **26**, 26 (2000).
10. N. Grandin, S. I. Reed, *Mol. Cell. Biol.* **13**, 2113 (1993).
11. Materials and Methods are available as supporting material on *Science* Online.
12. J. F. Charles *et al.*, *Curr. Biol.* **8**, 497 (1998).
13. M. Shirayama, W. Zachariae, R. Ciosk, K. Nasmyth, *EMBO J.* **17**, 1336 (1998).
14. F. Uhlmann, F. Lottspeich, K. Nasmyth, *Nature* **400**, 37 (1999).
15. S. B. Buonomo *et al.*, *Cell* **103**, 387 (2000).
16. S. M. Salah, K. Nasmyth, *Chromosoma* **109**, 27 (2000).
17. G. Alexandru, F. Uhlmann, K. Mechtler, M. A. Poupart, K. Nasmyth, *Cell* **105**, 459 (2001).
18. S. Keeney, C. N. Giroux, N. Kleckner, *Cell* **88**, 375 (1997).
19. A. Bergerat *et al.*, *Nature* **386**, 414 (1997).
20. A. J. Bardin, A. Amon, *Nature Rev. Mol. Cell. Biol.* **2**, 815 (2001).
21. F. Stegmeier, R. Visintin, A. Amon, *Cell* **108**, 207 (2002).
22. A. Marston, B. Lee, A. Amon, *Dev. Cell*, in press.
23. S. B. Buonomo *et al.*, *Dev. Cell*, in press.
24. C. Michaelis, R. Ciosk, K. Nasmyth, *Cell* **91**, 35 (1997).
25. X. He, S. Asthana, P. K. Sorger, *Cell* **101**, 763 (2000).
26. G. Goshima, M. Yanagida, *Genes Cells* **6**, 765 (2001).
27. T. Tanaka, J. Fuchs, J. Loidl, K. Nasmyth, *Nature Cell Biol.* **2**, 492 (2000).
28. B. H. Lee, A. Amon, S. Prinz, *Genes Dev.* **16**, 1672 (2002).
29. M. A. Shonn, R. McCarroll, A. W. Murray, *Genes Dev.* **16**, 1659 (2002).
30. B. H. Lee, unpublished observations.
31. O. Cohen-Fix, J. M. Peters, M. W. Kirschner, D. Koshland, *Genes Dev.* **10**, 3081 (1996).
32. T. Moll, G. Tebb, U. Surana, H. Robitsch, K. Nasmyth, *Cell* **66**, 743 (1991).
33. K. Nairz, F. Klein, *Genes Dev.* **11**, 2272 (1997).

34. We thank K. Nasmyth for strains and communication of results before publication and T. Orr-Weaver, F. Solomon, S. Prinz, and members of the Amon Lab for valuable input. This research was supported by NIH grant GM62207 (to A.A.) and a NSF predoctoral fellowship (to B.H.L.). A.A. is an investigator of the Howard Hughes Medical Institute.

Supporting Online Material

www.sciencemag.org/cgi/content/full/1081846/DC1
Materials and Methods
Figs. S1 to S6
Table S1
References

23 December 2002; accepted 18 March 2003
Published online 27 March 2003;
10.1126/science.1081846
Include this information when citing this paper.

Common Structure of Soluble Amyloid Oligomers Implies Common Mechanism of Pathogenesis

Rakez Kayed,[1] Elizabeth Head,[2] Jennifer L. Thompson,[1] Theresa M. McIntire,[3] Saskia C. Milton,[1] Carl W. Cotman,[2] Charles G. Glabe[1]*

Soluble oligomers are common to most amyloids and may represent the primary toxic species of amyloids, like the Aβ peptide in Alzheimer's disease (AD). Here we show that all of the soluble oligomers tested display a common conformation-dependent structure that is unique to soluble oligomers regardless of sequence. The in vitro toxicity of soluble oligomers is inhibited by oligomer-specific antibody. Soluble oligomers have a unique distribution in human AD brain that is distinct from fibrillar amyloid. These results indicate that different types of soluble amyloid oligomers have a common structure and suggest they share a common mechanism of toxicity.

Recent reports suggest that the toxicity of Aβ and other amyloidogenic proteins lies not in the insoluble fibrils that accumulate but rather in the soluble oligomeric intermediates (*1*). These soluble oligomers include spherical particles of 2.7 to 4.2 nm in diameter and curvilinear structures called "protofibrils" that appear to represent strings of the spherical particles (*2*). The oligomers have also been referred to as Aβ-derived diffusible ligands or ADDLs (*3*). The soluble Aβ oligomers represent protein micelles, because Aβ is an amphipathic surface-active peptide, oligomer formation displays a critical concentration dependence, and their formation is correlated with the appearance of a hydrophobic environment (*4–6*). Soluble Aβ oligomers are also found in human AD (Alzheimer's disease) cerebrospinal fluid (*7*), and the soluble Aβ content of human brain is better correlated with the severity of the disease than are plaques (*8–10*). Taken together, these results indicate that the soluble oligomers may be more important pathologically than are the fibrillar amyloid deposits, but there is no direct evidence that they actually exist in human AD brain. Here we report the production of an antibody that specifically recognizes micellar Aβ and not soluble, low–MW (molecular weight) Aβ or Aβ fibrils. To our surprise, this antibody also specifically recognizes soluble oligomers among all other types of amyloidogenic proteins and peptides examined, which indicates that they have a common structure and may share a common pathogenic mechanism as has been previously proposed (*11*).

To produce an antibody that specifically recognizes the oligomeric state of Aβ, we synthesized a molecular mimic of soluble oligomers on the basis of information about the organization of the Aβ within oligomers (fig. S1). The polyclonal serum produced by vaccination of rabbits with the molecular mimics is called oligomer-specific because it is specific for the soluble oligomeric intermediates and has no detectable reactivity with soluble low-MW or fibrillar Aβ species (Fig. 1, A and B). Unexpectedly, we observed no oligomer-specific immunoreactivity against low-MW Aβ or Aβ fibrils for the unfractionated serum even after boosting the rabbits 12 times, which indicates that the immune response to the molecular mimics is very specific.

Spherical oligomers are initially absent from freshly solubilized solutions of previ-

[1]Department of Molecular Biology and Biochemistry, University of California, Irvine, CA 92697–3900, USA. [2]Institute for Brain Aging & Dementia, University of California, Irvine, CA 92697–4540, USA. [3]Department of Chemistry, University of California, Irvine, CA 92697–2025, USA.
*To whom correspondence should be addressed. E-mail: cglabe@uci.edu

ously denatured Aβ and evolve over time, whereas spherical oligomer formation precedes the formation of the curvilinear strings or protofibrils (*12*). Therefore, we examined the kinetics of formation of oligomer-specific reactivity (Fig. 1C). For Aβ42, immunoreactivity is observed at 6 hours, is maximal between 24 and 168 hours, and then is not detected at 332 hours. The kinetics for Aβ40 are similar but are delayed by ~18 to 24 hours, consistent with previous observations that Aβ42 forms oligomers faster than does Aβ40 (*4*). We examined the samples by electron microscopy to determine the morphology and confirmed that at the early times of immunoreactivity, the samples contain predominantly spherical oligomers, whereas at later times the elongated "protofibrils" predominate. This observation indicates that both spherical and "protofibrillar" species display the same structure, one that is recognized by the antibody. We also examined the size dependence for the appearance of the epitope by fractionating soluble oligomers by size-exclusion chromatography (*4*). The smallest-sized oligomer that is recognized by oligomer-specific serum elutes at a position of ~40 kD, which corresponds to the approximate size of an octamer (Fig. 1D). Peaks eluting at positions corresponding to tetramer, dimer, and monomer are not reactive with oligomer-specific serum.

Spherical soluble oligomers have been observed for many different types of amyloids (*11*, *13*–*16*). We examined the specificity of oligomer-specific serum for soluble oligomers formed from a wide variety of amyloidogenic proteins and peptides by ELISA and dot blots. Surprisingly, the oligomer-specific antibody reacts well with all of the soluble oligomeric aggregates, regardless of sequence, and does not react with either the soluble low-MW species or the fibrils (Fig. 2A). This includes oligomeric and protofibrillar aggregates from α-synuclein, islet amyloid polypeptide (IAPP), polyglutamine, lysozyme, human insulin, and prion peptide 106-126. The oligomer-specific antibody does not detect any proteins in soluble lysates of SH-SY5Y cells (fig. S2). These results indicate that oligomer-specific antibody recognizes a unique common structural feature of the polypeptide backbone in the amyloid-soluble oligomers that is independent of the amino acid side chains.

Soluble oligomers have been implicated as the primary toxic species of amyloids (*2*, *3*, *11*, *17*). We examined whether oligomer-specific antibody could inhibit Aβ neurotoxicity in cell culture. Toxicity was assessed with 3-(4,5-dimethyl-2-thiazoyl)-2,5-diphenyltetrazolium bromide (MTT) reduction (Fig. 2B) and lactate dehydrogenase (LDH) release (fig. S3) assays in human neuroblastoma SH-SY5Y cells. Oligomer-specific antibody inhibited toxicity when Aβ soluble oligomers were incubated for 30 min with oligomer-specific antibody (Fig. 2B). Oligomer-specific antibody had no significant effect on the toxicity of Aβ fibrils. We also examined whether oligomer-specific antibody inhibits the toxicity of soluble oligomers formed by other amyloidogenic proteins and peptides. Oligomer-specific antibody also inhibits the toxicity mediated by all of the other types of soluble oligomers (Fig. 2C), and Fabs prepared from oligomer-specific immunoglobulin G (IgG) display equivalent inhibitory activity (fig. S3B). In contrast to Aβ, the fibrillar forms of the other amyloids do not display significant toxicity. A variety of control antibodies do not inhibit soluble Aβ oligomer toxicity (Fig. 2D). The observations that the soluble oligomeric forms of all of the amyloids display significant toxicity and that the toxicity is inhibited by oligomer-specific antibody suggest that they share a common structure that may mediate toxicity by a common mechanism.

We also examined the distribution of oligomer-specific immunoreactivity in human AD brain and normal age-matched controls.

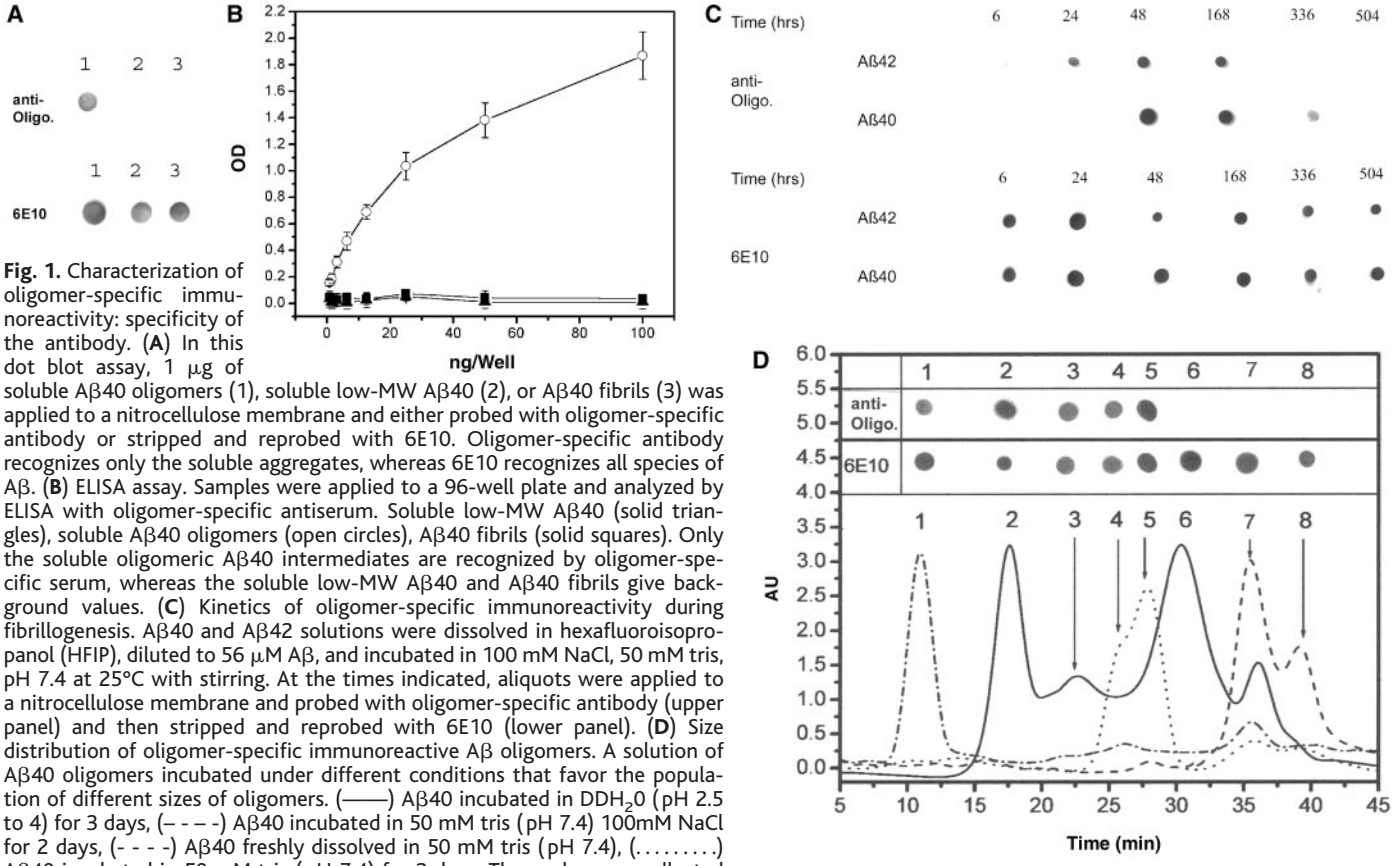

Fig. 1. Characterization of oligomer-specific immunoreactivity: specificity of the antibody. (**A**) In this dot blot assay, 1 μg of soluble Aβ40 oligomers (1), soluble low-MW Aβ40 (2), or Aβ40 fibrils (3) was applied to a nitrocellulose membrane and either probed with oligomer-specific antibody or stripped and reprobed with 6E10. Oligomer-specific antibody recognizes only the soluble aggregates, whereas 6E10 recognizes all species of Aβ. (**B**) ELISA assay. Samples were applied to a 96-well plate and analyzed by ELISA with oligomer-specific antiserum. Soluble low-MW Aβ40 (solid triangles), soluble Aβ40 oligomers (open circles), Aβ40 fibrils (solid squares). Only the soluble oligomeric Aβ40 intermediates are recognized by oligomer-specific serum, whereas the soluble low-MW Aβ40 and Aβ40 fibrils give background values. (**C**) Kinetics of oligomer-specific immunoreactivity during fibrillogenesis. Aβ40 and Aβ42 solutions were dissolved in hexafluoroisopropanol (HFIP), diluted to 56 μM Aβ, and incubated in 100 mM NaCl, 50 mM tris, pH 7.4 at 25°C with stirring. At the times indicated, aliquots were applied to a nitrocellulose membrane and probed with oligomer-specific antibody (upper panel) and then stripped and reprobed with 6E10 (lower panel). (**D**) Size distribution of oligomer-specific immunoreactive Aβ oligomers. A solution of Aβ40 oligomers incubated under different conditions that favor the population of different sizes of oligomers. (——) Aβ40 incubated in DDH_20 (pH 2.5 to 4) for 3 days, (– – – -) Aβ40 incubated in 50 mM tris (pH 7.4) 100mM NaCl for 2 days, (- - - -) Aβ40 freshly dissolved in 50 mM tris (pH 7.4), (. . . . . .) Aβ40 incubated in 50 mM tris (pH 7.4) for 2 days. The peaks were collected and dotted on a nitrocellulose membrane and probed with oligomer-specific antibody or 6E10 antibodies. The smallest oligomeric species that reacts with oligomer-specific antibody elutes with an apparent molecular weight of 40 kD, the size expected for an octamer.

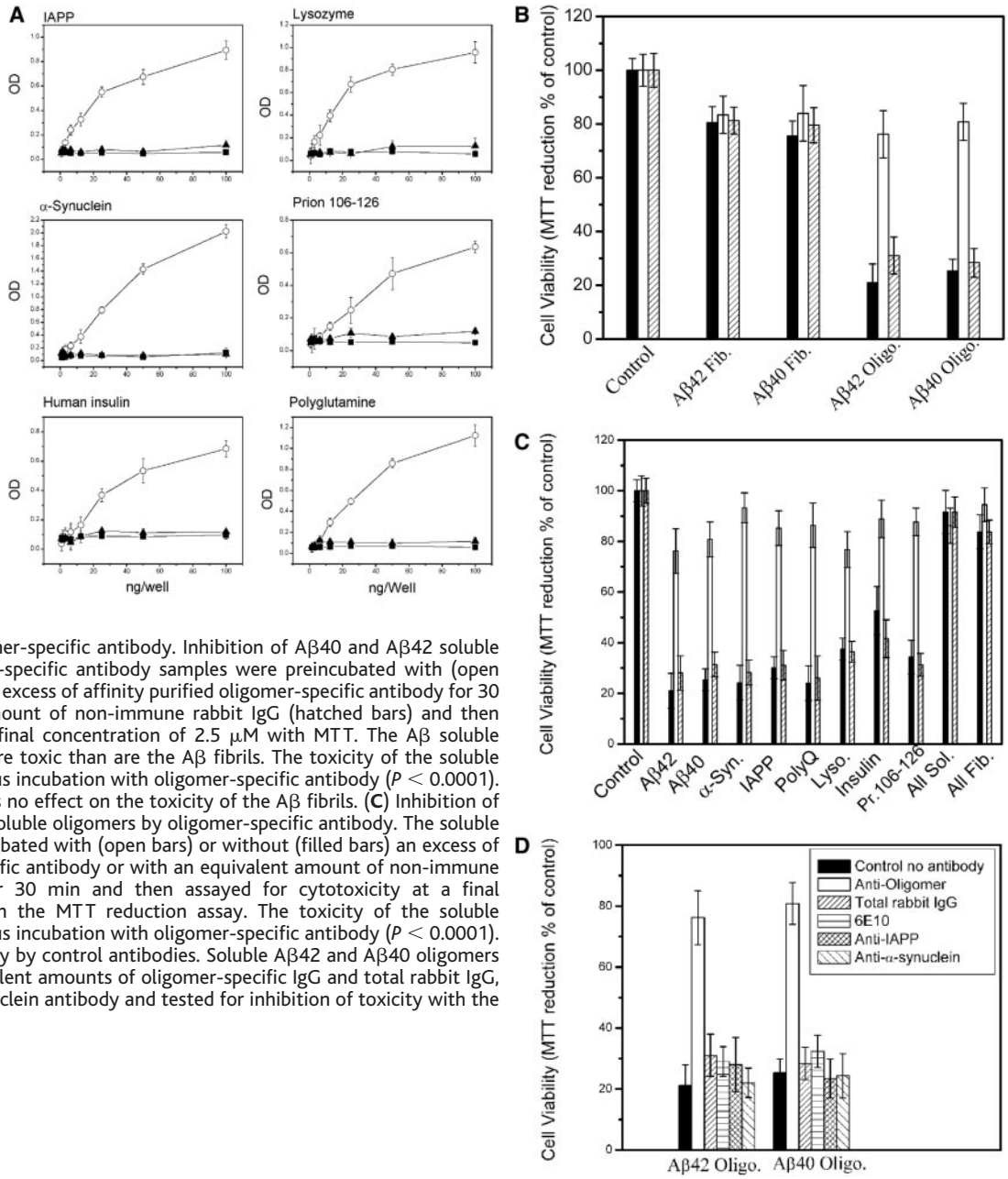

Fig. 2. Oligomer-specific antibody recognizes soluble oligomers of other types of amyloids and neutralizes their toxicity. (**A**) Soluble oligomers were prepared from a variety of other amyloid-forming proteins and peptides with no sequence homology, and their reactivity with oligomer-specific antibody was compared with the soluble and fibrils with an ELISA assay. Samples were applied to a 96-well plate and analyzed by ELISA with oligomer-specific antiserum. Soluble low-MW oligomers (solid triangles), soluble oligomers (open circles), fibrils (solid rectangles). Only the soluble oligomers are recognized by oligomer-specific serum, whereas the soluble low-MW oligomers and fibrils give background values. The type of amyloid is listed at the top of each panel. (**B**) Inhibition of the cytotoxicity of soluble oligomers by oligomer-specific antibody. Inhibition of Aβ40 and Aβ42 soluble oligomer toxicity by oligomer-specific antibody samples were preincubated with (open bars) or without (filled bars) an excess of affinity purified oligomer-specific antibody for 30 min or with an equivalent amount of non-immune rabbit IgG (hatched bars) and then assayed for cytotoxicity at a final concentration of 2.5 μM with MTT. The Aβ soluble oligomers are significantly more toxic than are the Aβ fibrils. The toxicity of the soluble oligomers is rescued by previous incubation with oligomer-specific antibody ($P < 0.0001$). Oligomer-specific antibody has no effect on the toxicity of the Aβ fibrils. (**C**) Inhibition of the toxicity of other types of soluble oligomers by oligomer-specific antibody. The soluble oligomer samples were preincubated with (open bars) or without (filled bars) an excess of affinity purified oligomer-specific antibody or with an equivalent amount of non-immune rabbit IgG (hatched bars) for 30 min and then assayed for cytotoxicity at a final concentration of 2.5 μM with the MTT reduction assay. The toxicity of the soluble oligomers is rescued by previous incubation with oligomer-specific antibody ($P < 0.0001$). (**D**) Lack of inhibition of toxicity by control antibodies. Soluble Aβ42 and Aβ40 oligomers were preincubated with equivalent amounts of oligomer-specific IgG and total rabbit IgG, 6E10, IAPP antibody, or α-synuclein antibody and tested for inhibition of toxicity with the MTT reduction assay.

Oligomer-specific immunoreactivity is observed as clusters of immunoreactive deposits distributed in the same regions of Aβ deposition in AD brain, but this distribution is spatially distinct and separate from the distribution of fibrillar Aβ deposits stained by thioflavin-S (Fig. 3A). Both small spherical puncta and larger curvilinear structures are labeled with oligomer-specific serum, where the larger structures appear to be arranged peripherally around diffuse deposits of smaller structures (Fig. 3C). No oligomer-specific antibody fluorescence was observed in association with neurofibrillary tangles, and virtually no oligomer-specific antibody staining was observed in control brain samples from individuals who were not demented, despite the presence of isolated cored Aβ plaques (Fig. 3B). Oligomer-specific antibody fails to detect any proteins on dot blots of lysates from normal nondemented human brain, but it detects oligomers in lysates from patients diagnosed with AD or "mild Braak changes," which may represent early changes associated with AD (fig. S4). The lack of background staining in control and AD tissue also indicates that oligomer-specific antibody does not react with β-amyloid precursor protein (APP). Occasionally oligomer-specific immunoreactivity is observed associated with relatively large 6E10-positive diffuse plaques (movie S1), but the 6E10 immunofluorescence does not overlap with the oligomer-specific immunofluorescence.

These results are direct evidence that oligomers exist as a distinct entity in human AD brain. The fact that most of these antibody-positive deposits are distinct from the thioflavin-S–positive amyloid deposits suggests that the deposits identified by oligomer-specific antibody are nonfibrillar and therefore may precede the development of fibrillar plaques. As such, they may represent the initial stage of amyloid deposition. Further, the relative amount of oligomer-specific antibody deposits is significantly lower than total Aβ, which suggests that these oligomers do not accumulate over time but may mature into fibrillar structures not detected by the oligomer-specific antibody.

Our observations with the oligomer-specific antibody indicate that oligomers

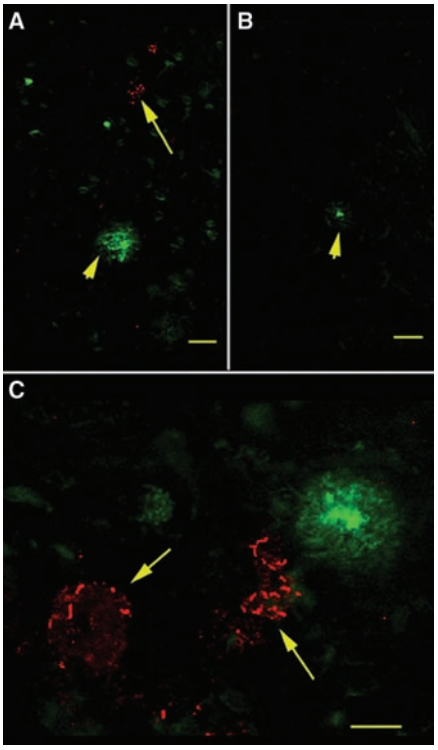

Fig. 3. Confocal immunofluorescence micrographs of human brain tissue. Sections from the entorhinal cortex of (**A**) an AD brain and (**B**) an age-matched control case were immunostained with oligomer-specific antibody (red) (arrows) and counterstained with thioflavin-S (green). Note the single thioflavin-S–positive plaque in the control case (arrowhead) and lack of oligomer-specific antibody fluorescence. (**C**) Oligomer-specific antibody positive deposits were observed in the AD case. When such deposits were found in association with a thioflavin-S–positive plaque, higher magnification and a Z-series indicated that the two deposits were spatially segregated. Scale bars, 20 μm.

have a conformation that is distinct from that of soluble monomers, low-MW oligomers, and fibrils. The fact that this epitope is common to amyloids of widely varying primary sequence further indicates that the epitope is formed from a specific conformation of the polypeptide backbone and is largely independent of the amino acid side chains in this region. A similar type of antibody specificity was recently reported by Wetzel and co-workers (*18*), but this antibody is specific for all types of amyloid fibrils and does not recognize soluble oligomers. Stefani and co-workers (*11*) have recently reported that soluble oligomers formed from non–disease-related proteins are inherently cytoxic, suggesting that they may have a common structure and function. Because the oligomer-specific antibody neutralizes the toxicity of oligomeric forms of all amyloids tested, they share a common structure, and they have a common mechanism of pathogenesis that is intimately associated with this common structure. This mechanistic commonality represents an important advance in our understanding of the mechanism of amyloid pathogenesis because it argues against a specific mechanism for one type of amyloid that is untenable for all of them. Because some amyloids, like Aβ, are in the extracellular space or the lumenal contents of the secretory and endocytic pathways, whereas other amyloids, like α-synuclein, reside in the cytosolic compartment, components that reside exclusively in either compartment are excluded as primary targets. In contrast, a common mechanism argues in favor of components that are accessible from both extracellular and cytosolic compartment, such as cell membranes as primary targets of amyloid pathogenesis.

References and Notes

1. J. Hardy, D. J. Selkoe, *Science* **297**, 353 (2002).
2. D. M. Hartley *et al.*, *J. Neurosci.* **19**, 8876 (1999).
3. M. P. Lambert *et al.*, *Proc. Natl. Acad. Sci. U.S.A.* **95**, 6448 (1998).
4. B. Soreghan, J. Kosmoski, C. Glabe, *J. Biol. Chem.* **269**, 28551 (1994).
5. L. O. Tjernberg *et al.*, *Chem. Biol.* **6**, 53 (1999).
6. H. LeVine, 3rd, *Arch. Biochem. Biophys.* **404**, 106 (2002).
7. M. Pitschke, R. Prior, M. Haupt, D. Riesner, *Nature Med.* **4**, 832 (1998).
8. Y. M. Kuo *et al.*, *J. Biol. Chem.* **271**, 4077 (1996).
9. C. A. McLean *et al.*, *Ann. Neurol.* **46**, 860 (1999).
10. L. F. Lue *et al.*, *Am. J. Pathol.* **155**, 853 (1999).
11. M. Bucciantini *et al.*, *Nature* **416**, 507. (2002).
12. J. D. Harper, S. S. Wong, C. M. Lieber, P. T. Lansbury Jr., *Biochemistry* **38**, 8972 (1999).
13. K. A. Conway, J. D. Harper, P. T. Lansbury Jr., *Biochemistry* **39**, 2552 (2000).
14. C. Goldsbury, J. Kistler, U. Aebi, T. Arvinte, G. J. Cooper, *J. Mol. Biol.* **285**, 33 (1999).
15. T. R. Serio *et al.*, *Science* **289**, 1317 (2000).
16. O. M. El-Agnaf, S. Nagala, B. P. Patel, B. M. Austen, *J. Mol. Biol.* **310**, 157 (2001).
17. H. A. Lashuel, D. Hartley, B. M. Petre, T. Walz, P. T. Lansbury Jr., *Nature* **418**, 291. (2002).
18. B. O'Nuallain, R. Wetzel, *Proc. Natl. Acad. Sci. U.S.A.* **99**, 1485. (2002).
19. This work was supported by NIH grants NS31230, AG00538, and AG16573 and by a grant from the Larry L. Hillblom foundation. We are grateful to D. A. Brant, Department of Chemistry, University of California, Irvine, for his support; R. Wetzel for providing the polyglutamine peptide; F. Saroza for technical assistance; and R. Langen for providing α-synuclein. R.K. thanks K. Sweimeh and Y. Al-Abed for helpful discussions.

Supporting Online Material

www.sciencemag.org/cgi/content/full/300/5618/486/DC1
Materials and Methods
SOM Text
Figs. S1 to S4
References
Movie S1

16 October 2002; accepted 21 March 2003

Induction of Tumors in Mice by Genomic Hypomethylation

François Gaudet,[1,2,3] J. Graeme Hodgson,[4] Amir Eden,[1] Laurie Jackson-Grusby,[1] Jessica Dausman,[1] Joe W. Gray,[4] Heinrich Leonhardt,[2,3] Rudolf Jaenisch[1]*

Genome-wide DNA hypomethylation occurs in many human cancers, but whether this epigenetic change is a cause or consequence of tumorigenesis has been unclear. To explore this phenomenon, we generated mice carrying a hypomorphic DNA methyltransferase 1 (*Dnmt1*) allele, which reduces Dnmt1 expression to 10% of wild-type levels and results in substantial genome-wide hypomethylation in all tissues. The mutant mice were runted at birth, and at 4 to 8 months of age they developed aggressive T cell lymphomas that displayed a high frequency of chromosome 15 trisomy. These results indicate that DNA hypomethylation plays a causal role in tumor formation, possibly by promoting chromosomal instability.

Human cancer cells often display abnormal patterns of DNA methylation. The role of aberrant hypermethylation in the silencing of tumor suppressor genes is now well documented (*1*). In contrast, the role of aberrant hypomethylation—which is observed in a wide variety of tumors (*2*–*5*), often together with regional hypermethylation—has remained unclear.

To investigate whether DNA hypomethylation has a causal role in tumor formation, we generated mice with highly reduced levels of Dnmt1, the enzyme that maintains DNA methylation patterns in somatic cells (*6*). Because mice homozygous for a Dnmt1 null allele ($Dnmt1^{c/c}$) die during gestation (*7, 8*), we combined a hypomorphic allele [$Dnmt1^{chip}$ (*9*)] with a null allele to generate $Dnmt1^{chip/c}$ (referred to here as $Dnmt1^{chip/-}$) compound heterozygotes with a substantially reduced level of genome-wide DNA methyl-

[1]Whitehead Institute for Biomedical Research and Department of Biology, Massachusetts Institute of Technology, Cambridge, MA 02142, USA. [2]Ludwig Maximilians University, Department of Biology II, 80336 Munich, Germany. [3]Max Delbrück Center for Molecular Medicine, 13125 Berlin, Germany. [4]Department of Laboratory Medicine and UCSF Comprehensive Cancer Center, University of California, 2340 Sutter Street, San Francisco, CA 94143, USA.

*To whom correspondence should be addressed. E-mail: jaenisch@wi.mit.edu